CHAPTER 5

STABILITY AND FAILURE OF SUDDENLY LOADED LAMINATED COMPOSITE CYLINDRICAL PANEL

5.1 Introduction

In the previous chapter, the stability and failure of laminated composite plate subjected to in-plane pulse loads was investigated. In this chapter, the dynamic buckling behaviour of laminated composite cylindrical panel is investigated. The first ply failure load is also calculated to check if the dynamic buckling is occurring before or after the first ply failure load. First, the convergence study and validation study are presented and then the results of the investigation are presented. The influence of various parameters such as loading duration, loading function, aspect ratio, curvature, stacking sequence and boundary conditions on the dynamic buckling behaviour of the panel are investigated. The chapter is divided into following subsections:

- Convergence and Validation Studies
    - Convergence and Validation of Static buckling Load of a Composite Cylindrical Panel
    - Convergence of Dynamic Load
- Dynamic Buckling Studies
    - Effect of Loading Duration
    - Failure of Cylindrical Panel
    - Effect of Aspect Ratio
    - Effect of Curvature
    - Effect of Loading Function
    - Effect of Boundary Conditions
- Shock Spectrum of a Cylindrical Panel

5.2 Convergence and Validation Studies

In this section, the results of convergence and validation study of a laminated composite cylindrical panel are presented. The validation studies are carried out for static buckling load and dynamic load.

5.2.1 Convergence and Validation studies of static buckling load of a composite cylindrical panel

The static buckling load of a cylindrical panel is evaluated and validated using the results from the literature in this section. Non-dimensional static buckling load is calculated for a square planed cylindrical panel with stacking sequence (0°/90°/0°/90°/0°). The geometry of the plate is shown in Fig. 3.6. The pre-buckling boundary conditions are shown in Fig. 5.1. The boundary conditions for buckling analysis are shown in Fig. 3.7(a). The material properties and other parameters are taken as: b/a = 1, R/a = 20, $E_{11} = 40E_{22}$, $G_{12} = G_{13} = 0.5E_{22}$, $G_{23} = 0.6E_{22}$ and ν_{12} = 0.25 as reported by Di Sciuva and Carrera (1990). The non-dimensional static buckling load is calculated using Eqn. (5.1) where 'a' is the length of the loaded edge and 'h' is the thickness of the panel.

$$\overline{P_{cr}} = \frac{P_{cr}\, b^2}{E_{22} h^3} \tag{5.1}$$

Figure 5.2(a) shows the convergence study of the non-dimensional static buckling loads for the panel of b/h = 100 for various mesh sizes. The non-dimensional static buckling loads of the present study are compared with the finite element results of Di Sciuva and Carrera (1990) and Patel *et al.* (2003) in Table 5.1. The error shown in the table is with respect to the result reported by Di Sciuva and Carrera (1990).

Table 5.1 Non-dimensional static buckling load for a panel with b/a=1, b/h=100, R/a=20 and stacking sequence (0°/90°/0°/90°/0°).

Analysis	Mesh size	Non-dimensional static buckling load
Di Sciuva and Carrera (1990)	5 × 5	36.86
Patel *et al.* (2003)	8 × 8	36.84
Present	50 × 50	36.4735
Error (%)	-	1.05

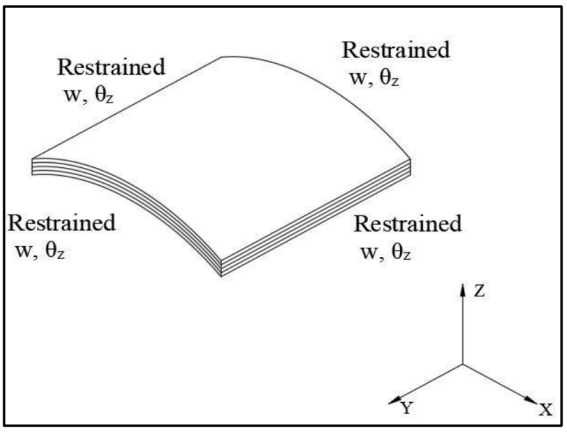

Fig. 5.1 Pre-buckling boundary conditions for a composite cylindrical panel

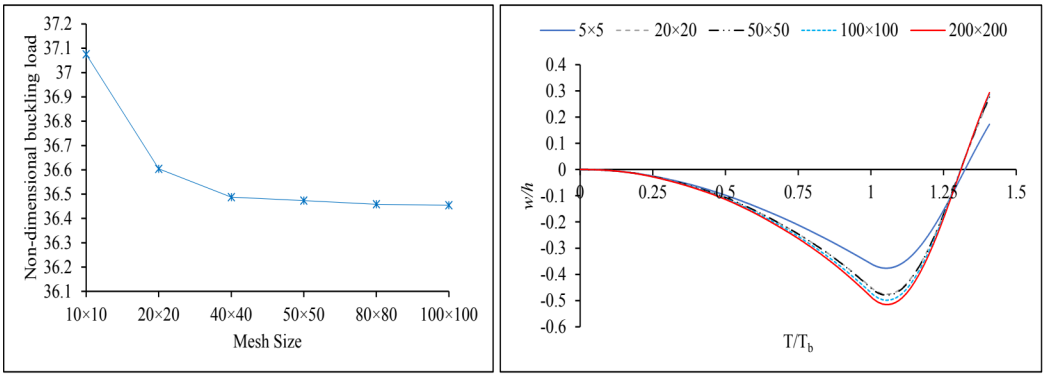

(a) **(b)**

Fig. 5.2 Convergence study of a laminated composite cylindrical panel **(a)** Non-dimensional static buckling load **(b)** Dynamic load

From Fig. 5.2(a) it is seen that the static buckling load is converged at mesh size 50×50. From Table 5.1, it is seen that the result of the static buckling load convergence study with mesh size 50×50 match with the results from the literature.

5.2.2 Convergence of dynamic load

The results of the convergence study of the dynamic loading on a cylindrical panel is presented in this section. For performing dynamic analysis, formation of mass matrix is necessary, so the material properties presented by Priyadarsini *et al.* (2012) are used. E_{22} = 9250 MPa and ρ=1700 Kg/m^3. For dynamic convergence study, the panel with the material and geometric

properties mentioned in the previous section is subjected to dynamic load equal to static buckling load (337.38 kN/m) in the form of rectangular in-plane pulse load (Fig. 3.5(a)) till its first natural period (T_b=14.206×10^{-3}s). The transverse displacement is calculated for different mesh sizes. The convergence study on dynamic load is presented in Fig. 5.2(b). From Fig. 5.2(b) it is observed that, the transverse displacement is converged at a mesh size of 50×50. The denser the mesh, the longer it takes for the completion of analysis. So, the mesh sizes of 100×100 and 200×200 are time consuming.

From the convergence and validation study, it is observed that the results of the present study match well with the results from the literature. The same mesh size (50×50) is used in the dynamic buckling studies. The same boundary conditions for the pre-buckling and the buckling stage, as was the case in dynamic buckling analysis of the plate.

5.3 Dynamic Buckling Studies

In this section, the results of the dynamic buckling studies and the failure studies are presented. The procedure for calculating the dynamic buckling were presented in the previous chapter (section 4.3). The same procedure is used for the case of laminated composite cylindrical panel.

In Fig. 5.3, the plot of non-dimensional time vs non-dimensional displacements for a panel with *b/a*=1, *b/h*=100, *R/a*=5 and stacking sequence (0°/90°/90°/0°) is shown. The panel is subjected to rectangular in-plane pulse load till its first natural period and the displacements are observed after the removal of the load. The non-dimensional time vs failure index with respect to Tsai-Wu failure criterion in plotted in Fig. 5.4 for a panel with *b/a*=1, *a/h*=100, *R/a*=5 and stacking sequence (0°/90°/90°/0°), subjected to rectangular pulse load.

In Fig. 5.5, the non-dimensional load vs non-dimensional displacement for a composite cylindrical panel with *b/a*=1, *a/h*=100, *R/a*=5 and stacking sequence (0°/90°/90°/0°) subjected to rectangular pulse load is shown along with the deformed shape of the panel at different magnitude of loads. In Fig. 5.6, the non-dimensional load vs failure index with respect to Tsai-Wu failure criterion for a composite cylindrical panel with *b/a*=1, *a/h*=100, *R/a*=5 and stacking sequence (0°/90°/90°/0°) subjected to rectangular pulse load is shown along with the deformed shape of the panel at different magnitude of loads. In Fig, 5.5, region in blue colour represents

the region with maximum displacement and in Fig. 5.6, region in red colour represents the region with maximum failure index with respect to Tsai-Wu failure criterion.

The scale factor for the deformed shape of the panel is 7 in both Fig. 5.5 ad Fig. 5.6. It is observed from Fig. 5.3 and Fig. 5.4 that the maximum displacement and the maximum failure index can occur after the removal of the pulse load. Thus, it is essential to evaluate the response of the panel after the removal of the load as well. It is also observed that the dynamic buckling load of the panel is lower than the static buckling and also its first ply failure load.

In Fig. 5.5 it is observed from that the location of maximum deformation does not change with the change in the magnitude of the load. In Fig. 5.6, it is observed that the location of maximum failure index changes from the centre of the panel to the region near the loading edges at first ply failure load. Further, the influence of loading duration, loading function, stacking sequence, aspect ratio of the panel, curvature of the panel and the boundary conditions on the dynamic buckling behavior of the laminated composite cylindrical panel is investigated and the results are presented in the following sections.

In each section, the static load (N_{st}) is the static buckling load of the panel considered. So, the ratio N_{dyn}/N_{st} is unique for each plot. Comparison is made with respect to the dynamic performance of the panel with respect to the static buckling load for each case. By this, in each case it can be checked if the panel has sufficient strength and stiffness to resist in-plane pulse load in place of static load. The static buckling load and the first natural period of the panels considered for the study are presented in Table 5.2. The laminated composite cylindrical panel with a/h=100 and a=0.1m is considered for various radius of curvatures and ply orientations. The various boundary conditions are shown in Fig. 3.7(a)-Fig. 3.7(d).

Table 5.2 Static buckling load and first natural period of the cylindrical panel with a/h=100 and a=0.1m for various radius of curvatures and ply orientations

R/a	*b/a*	Boundary Condition	Stacking Scheme	Static Buckling Load (N/m)	First Natural Period (s)
5	1	BC1	(0°/90°/90°/0°)	30848	1.41×10-3
5	1.5	BC1	(0°/90°/90°/0°)	31932	1.85×10-3
5	2	BC1	(0°/90°/90°/0°)	33519	2.12×10-3
5	2.5	BC1	(0°/90°/90°/0°)	34750	2.28×10-3

(Table 5.2 Continued)

5	3	BC1	(0°/90°/90°/0°)	35642	2.38×10-3
5	1	BC1	(45°/-45°/-45°/45°)	45934	8.42×10-4
5	1.5	BC1	(45°/-45°/-45°/45°)	52330	1.5×10-3
5	2	BC1	(45°/-45°/-45°/45°)	56393	2.29×10-3
5	2.5	BC1	(45°/-45°/-45°/45°)	58260	2.9×10-3
5	3	BC1	(45°/-45°/-45°/45°)	58888	3.32×10-3
10	1	BC1	(0°/90°/90°/0°)	18212	1.9×10-3
10	1	BC1	(45°/-45°/-45°/45°)	30949	1.32×10-3
5	1	BC2	(0°/90°/90°/0°)	53968	5.1×10-4
5	1	BC3	(0°/90°/90°/0°)	42358	9.92×10-4
5	1	BC4	(0°/90°/90°/0°)	10057	2.6×10-3
5	1	BC2	(45°/-45°/-45°/45°)	73540	6.87×10-4
5	1	BC3	(45°/-45°/-45°/45°)	54211	7.99×10-4
5	1	BC4	(45°/-45°/-45°/45°)	14627	2.14×10-3

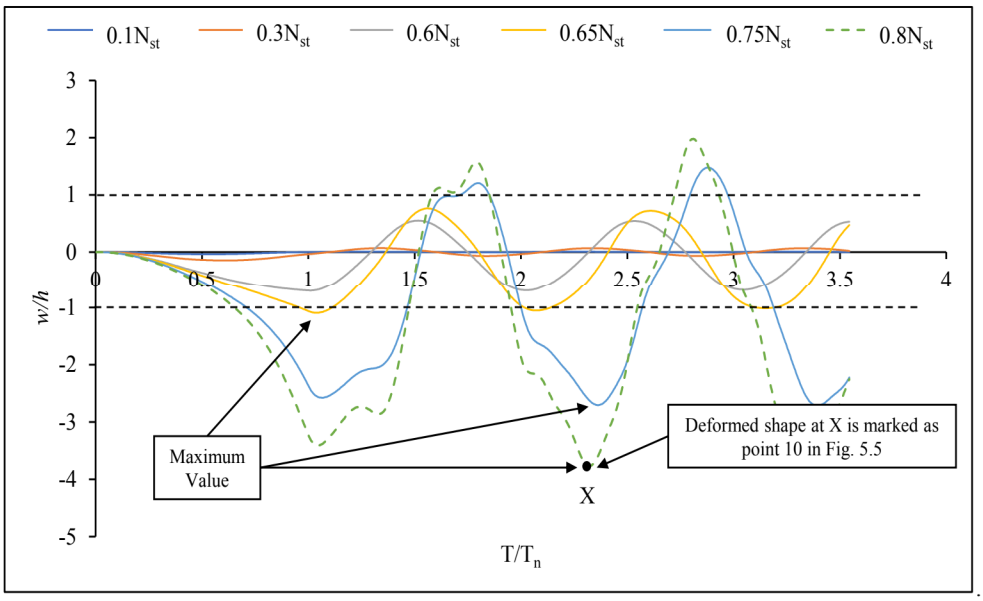

Fig. 5.3 Non-Dimensional Time vs non-dimensional Displacement for a panel with *b/a*=1, *a/h*=100, *R/a* =5 and stacking sequence (0°/90°/90°/0°) when subjected to various magnitudes of rectangular pulse load.

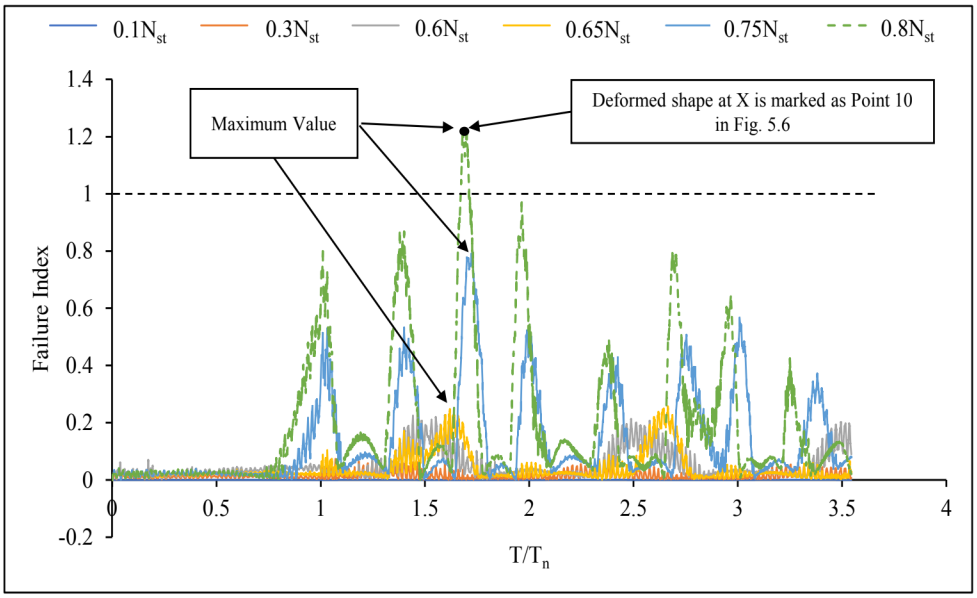

Fig. 5.4 Non-Dimensional Time vs Failure Index (Tsai-Wu criterion) for a panel with *b/a*=1, *a/h* =100, *R/a* =5 and stacking sequence (0°/90°/90°/0°) when subjected to various magnitudes of rectangular pulse load.

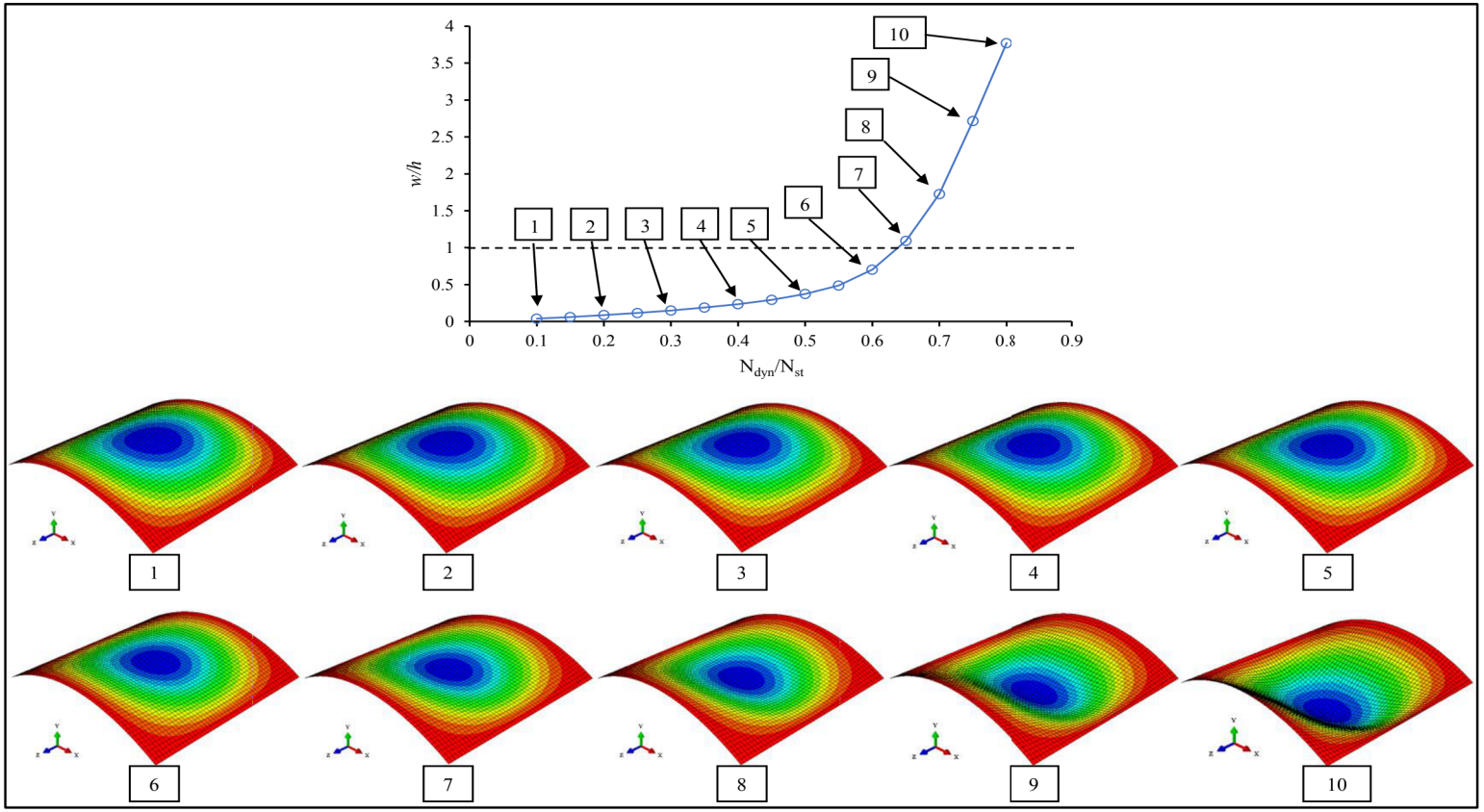

Fig. 5.5 Non-dimensional load vs non-dimensional Displacement for the panel with *b/a*=1, *a/h*=100, *R/a* =5 and stacking sequence (0°/90°/90°/0°) when subjected to rectangular pulse load along with the deformed shape of the panel at various magnitude of loads. Scale Factor=7.

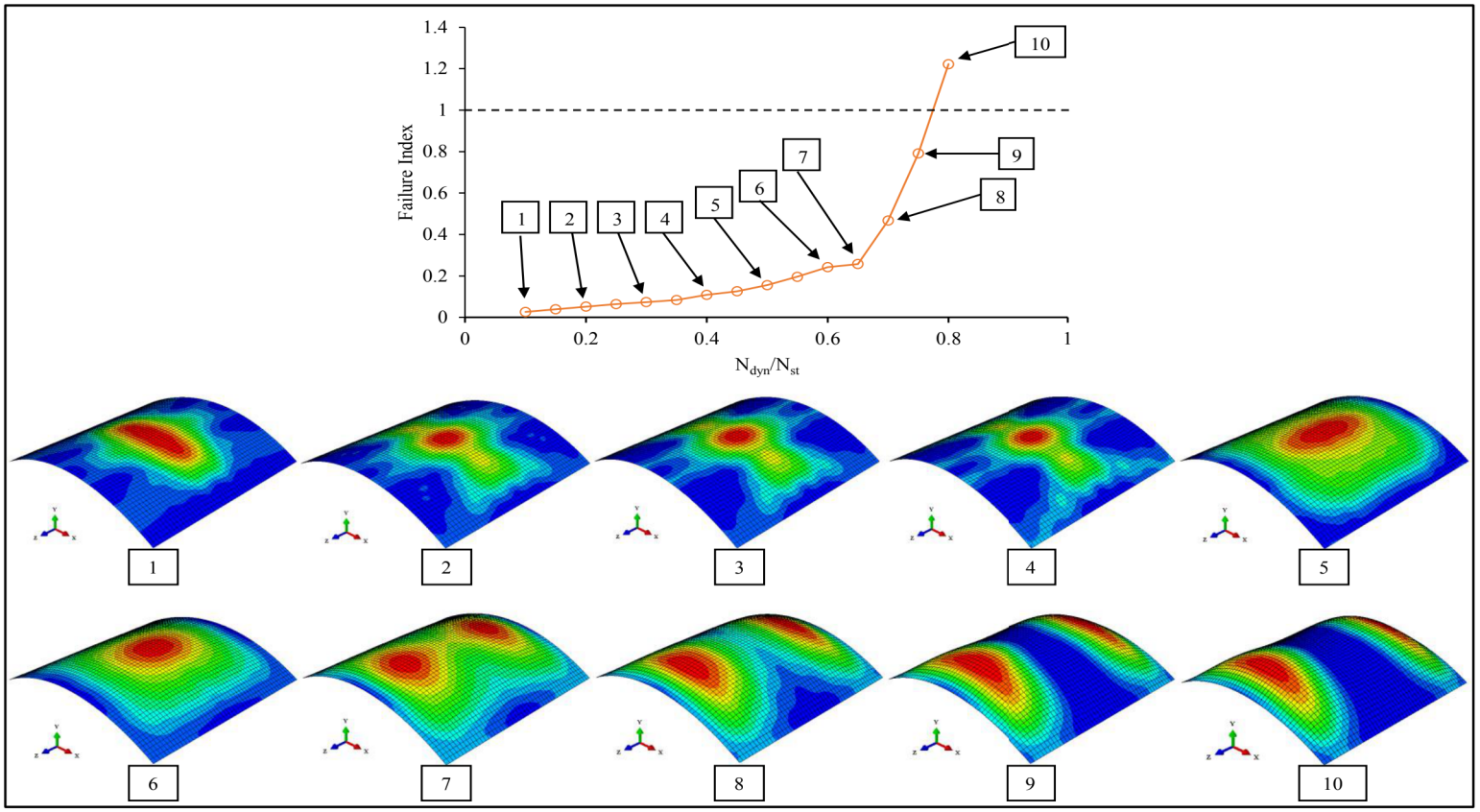

Fig. 5.6 Non-dimensional Load vs Failure Index (Tsai-Wu criterion) for the panel with *b/a*=1, *a/h*=100, *R/a* =5 and stacking sequence (0°/90°/90°/0°) when subjected to rectangular pulse load along with the deformed shape of the panel at various magnitude of loads. Scale Factor=7.

5.3.1 Effect of loading duration

In this section, the effect of loading duration on the stability and first ply failure of a laminated composite cylindrical panel subjected to in-plane pulse load is presented. For this study, a cylindrical panel with dimensions *b/a*=1, *R/a*=5, *a/h*=100, stacking sequence (0°/90°/90°/0°) are considered. The panel is loaded with both rectangular and sinusoidal pulse loading functions. The ratios of applied loading duration (T_b) to first natural period (T_n) considered are ⅕, ⅖, 2.5, and 5. Figure 5.7(a) shows the plot of non-dimensional load vs non-dimensional displacement for a panel with, *b/a*=1, *R/a*=5, *a/h*=100; subjected to rectangular pulse load. Figure 5.7(b) shows the plot of non-dimensional load vs non-dimensional displacement for a panel with, *b/a*=1, *R/a*=5, *b/h*=100; subjected to sinusoidal pulse load.

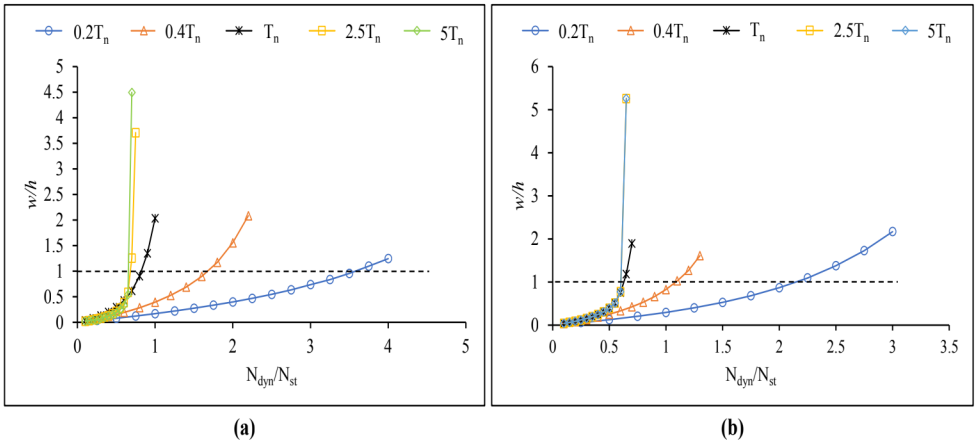

Fig. 5.7 Non-dimensional Load vs non-dimensional Displacement for a panel with *b/a*=1, *R/a*=5, *a/h*=100, stacking sequence (0°/90°/90°/0°) for various loading durations **(a)** subjected to sinusoidal pulse load **(b)** subjected to rectangular pulse load

It is seen from Fig.5.7, that the loading duration near the first natural period is critical irrespective of the loading function. A sharp increase in displacement is observed at N_{dyn}/N_{st} =0.6−0.7, showing a critical point of instability in the panel. In section 4.2.2, it was shown that the peak response of an isotropic plate is observed near the first natural period of the plate. From the conclusions drawn from the Fig. 5.7(a) and Fig. 5.7(b), for the rest of the study, the panel is loaded till its time of first natural period and the maximum transverse displacements are observed. The first natural period is an inherent property of any structural component. If the structural component is subjected to dynamic load having the period equal to its first natural

period, then the component will show larger displacements compared to loads for a duration much lower than it. It is similar to the example of earthquake with a particular period hitting a city. The buildings which are having their first natural same as that of the earthquake period will show large response. The results presented in Fig. 5.7 also signify that the stiffness of the panel changes with the change in duration of loading which results in change in dynamic buckling load Panels exhibit a higher stiffness when subjected to an in-panel pulse load for a duration much lower than its first natural period.

5.3.2 Failure of cylindrical panel

In this section, the first ply failure of laminated composite cylindrical panel subjected to in-plane pulse load is investigated. A panel with *b/a*=1, *R/a*=5, *b/h*=100 and stacking sequence (45°/−45°/−45°/45°) is subjected to rectangular pulse load. Simply supported boundary conditions are considered for the panel. Figure 5.8(a) shows the plot of non-dimensional load vs non-dimensional displacement for panel with *R/a*=5 and stacking sequence (45°/−45°/−45°/45°). Figure 5.8(b) shows the plot of non-dimensional load vs failure index with respect to various failure theories for panel with *R/a*=5 and stacking sequence (45°/−45°/−45°/45°).

The variation of stress and strain with respect to time is studied. For this, the node at the center (Node 1301) at the bottommost surface of the cylindrical panel, marked in Fig.5.9 is considered. This point is selected because the failure index zone is maximum at this location. The dynamic loading magnitude (N_{dyn}/N_{st}) is 0.7. The plots of true stress (σ_{XX}) vs non-dimensional time and logarithmic strain (ϵ_{XX}) vs non-dimensional time are shown in Fig.5.10(a) and Fig. 5.10(b) respectively. An element (1226) is chosen and the results are shown for one of the nodes (1301) of this element. Further, at this maximum failure index location the failure index is calculated at each layer of the panel to find out which layer is failing during the first ply failure analysis. The failure index for layer 1 is 1.626, for layer 2 is 0.8106, for layer 3 is 0.732 and for layer 4 is 1.123. The numbering of layers starts from the bottom to top in increasing Z-direction. So, for this particular case during the first ply failure analysis, the bottommost layer is failing first.

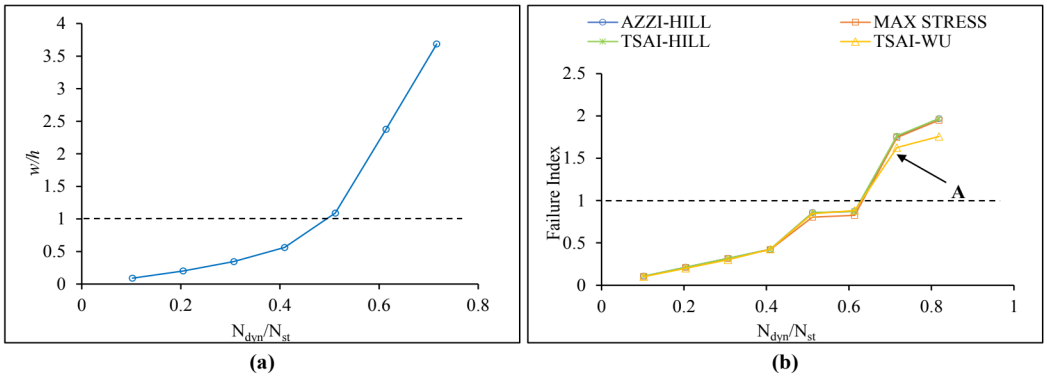

Fig. 5.8 Plot for laminated composite cylindrical panel with *b/a*=1, *R/a*=5, *a/h*=100, stacking sequence (45°/−45°/−45°/45°) subjected to rectangular pulse load. **(a)** Non-dimensional Load vs non-dimensional Displacement **(b)** Non-dimensional Load vs Failure index

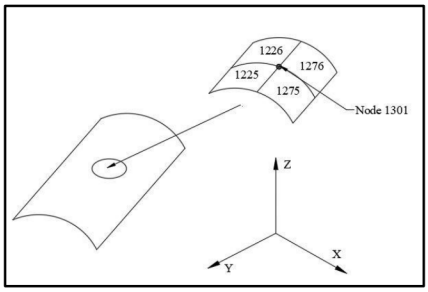

Fig. 5.9 Location of node at which the variation of stress and strain with respect to time is observed in Fig. 5.10(a) and Fig. 5.10(b) respectively.

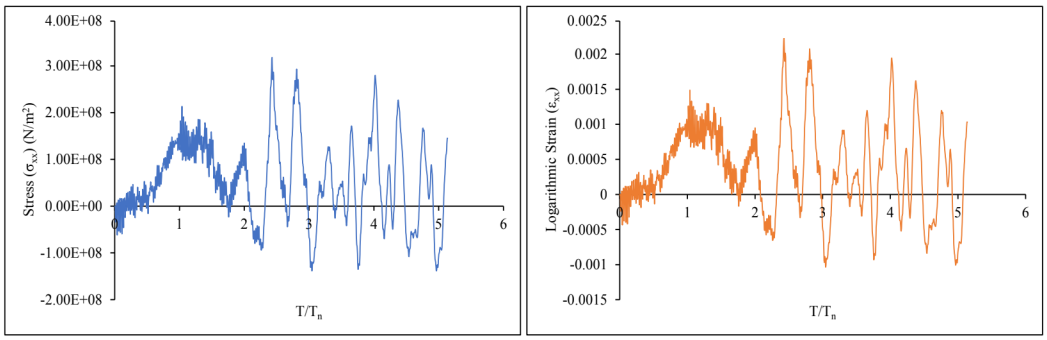

Fig. 5.10 Plot for a laminated composite cylindrical panel with *b/a*=1, *R/a*=5, *a/h*=100, stacking sequence (45°/−45°/−45°/45°) subjected to rectangular pulse load corresponding to point A in Fig. 5.8(b) **(a)** True Stress (σ_{XX}) vs non-dimensional Time **(b)** Logarithmic Strain (ε_{XX}) vs non-dimensional Time

It is seen from the Fig. 5.8(a) that the nonlinear dynamic buckling load of the panel is much less than its static buckling load. The dynamic buckling load with respect to Vol'mir's criterion is around 50% lower than its static buckling load. From the Fig. 5.8(b) it is seen that the first ply failure of the panel is occurring after the panel has buckled due to rectangular in-plane pulse load. It is also observed that the Tsai-Wu failure criterion gives slightly lower value of failure index as it is much more interactive failure theory. It is also observed that the maximum true stress and the maximum logarithmic strain in the panel occur after the removal of the load. This observation along with the observations from Fig. 5.3 and Fig. 5.4 signify that, when a cylindrical panel is subjected to dynamic pulse load, it is necessary to calculate the deformations and the stresses after the removal of the load as well.

5.3.3 Effect of aspect ratio

The effect of aspect ratio on the dynamic buckling behaviour of a laminated composite cylindrical panel subjected to in-plane pulse load is investigated in this section. The ratio *b/a* is varied, keeping *a* constant. For this study, both cross-ply and angle-ply laminates are considered. The panel is subjected to rectangular and sinusoidal in-plane pulse loading functions. Figure 5.11(a) shows the plot of non-dimensional load vs non-dimensional displacement for a cylindrical panel with, *R/a*=5, *a/h*=100, stacking sequence (45°/−45°/−45°/45°); subjected to rectangular loading function. Figure 5.12(b) shows the plot of non-dimensional load vs non-dimensional displacement for a cylindrical panel with, *R/a*=5, *b/h*=100, stacking sequence (0°/90°/90°/0°); subjected to rectangular loading function. Figure 5.12(a) shows the plot of non-dimensional load vs non-dimensional displacement for a cylindrical panel with, *R/a*=5, *a/h*=100, stacking sequence (45°/−45°/−45°/45°); subjected to sinusoidal loading function. Figure 5.12(b) shows the plot of non-dimensional load vs non-dimensional displacement for a cylindrical panel with, *R/a*=5, *b/h*=100, stacking sequence (0°/90°/90°/0°); subjected to sinusoidal pulse load.

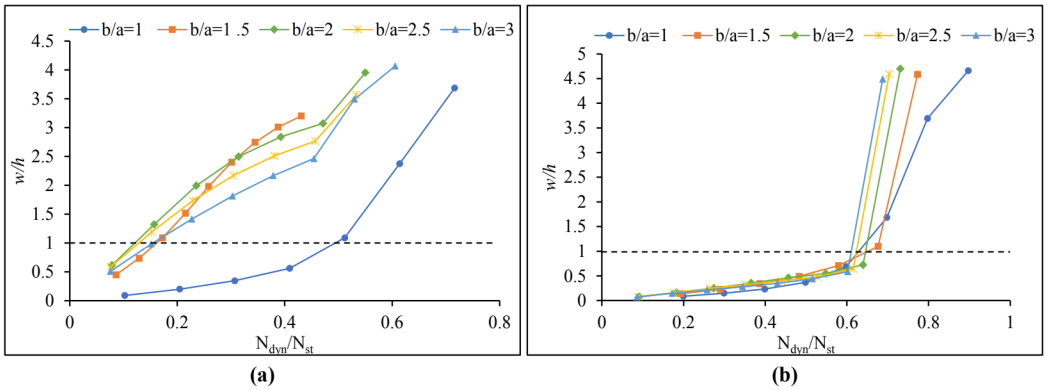

Fig. 5.11 Non-dimensional Load vs non-dimensional Displacement of a cylindrical panel with *R/a*=5 and *a/h*=100 subjected to rectangular pulse load for various aspect ratios. **(a)** stacking sequence is (45°/−45°/−45°/45°) **(b)** stacking sequence is (0°/90°/90°/0°)

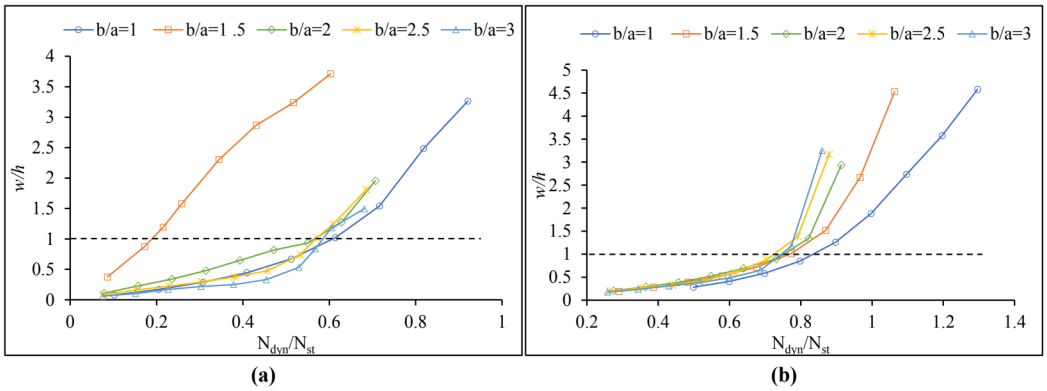

Fig. 5.12 Non-dimensional Load vs non-dimensional Displacement of a cylindrical panel with *R/a*=5 and *a/h*=100 subjected to sinusoidal pulse load for various aspect ratios. **(a)** stacking sequence is (45°/−45°/−45°/45°) **(b)** stacking sequence is (0°/90°/90°/0°)

In Fig. 5.11 and Fig. 5.12, N_{st} changes with the change in *b/a* ratio. This means that each plot is unique, and the dynamic performance of each panel is compared to its static buckling load. In Fig. 5.11 it is observed that the panel when subjected to in-plane pulse load with rectangular loading function till its first natural period, its dynamic buckling load is lower than its respective static buckling load. In Fig. 5.11(a), the panel with *b/a*=1 has a dynamic buckling load 50% lower than its static buckling load and for the rest of the cases, it is 84%-88% lower than their respective static buckling loads. In Fig. 5.11(b), the panel with various aspect ratios have dynamic buckling loads 35%-38% lower than their respective static buckling loads. In

Fig. 5.12(a), the panel with *b/a*=1.5 has significantly lower dynamic buckling load (80%) than its static buckling load. For the rest of the cases, the dynamic buckling loads of the panels are 40%-44% lower than their respective static buckling loads. The reason for this anomaly is that the panel when subjected to in-plane pulse load, has the tendency to deform in a shape of its first buckling mode. With the increase in the aspect ratio of the panel, the number of half cycles of sine series increases. The change in shape of first buckling mode of the cylindrical panel for the *b/a*=1.5 and for panels with *b/a* >1.5 could be one of the reasons for this behavior. In Fig. 5.12(b) the dynamic buckling of the panel is 16%-24% lower than its respective static buckling load. These results signify that the stiffness of thin composite panel with lower curvature (*R/a*=5) having cross-ply or angle ply laminates is much lower when subjected to in-plane pulse loads till their respective first natural periods than the panels when subjected to static loads.

These results signify that the panel which is designed for static loads it not capable of resisting dynamic in-plane pulse loads which are of either of rectangular loading function or sinusoidal loading function. This observation is valid for thin panel with either balanced and symmetric cross-ply or angle ply laminates when the radius of curvature of the panel is small (*R/a* =5) which could vary with the variation in the curvature of the panel.

5.3.4 Effect of curvature

The influence of curvature on the dynamic buckling behaviour of panel subjected to in-plane pulse load is studied in this section. The aspect ratio and thickness of the laminated composite cylindrical panel are kept constant and the ratio *R/a* is varied. Two values are considered: *R/a*=5 and 10 for cross-ply and angle-ply panels subjected to rectangular pulse load and sinusoidal pulse load. Figure 5.13(a) shows the plot of non-dimensional load vs non-dimensional displacement for a panel with, *b/a*=1, *b/h*=100, stacking sequence (45°/−45°/−45°/45°) and (0°/90°/90°/0°); subjected to rectangular pulse load. Figure 5.13(b) shows the plot of non-dimensional load vs Failure index with respect to Tsai-Wu failure criterion for a panel with, *b/a*=1, *b/h*=100, stacking sequence (45°/−45°/−45°/45°) and (0°/90°/90°/0°); subjected to rectangular pulse load. Figure 5.14(a) shows the plot of non-dimensional load vs non-dimensional displacement for a panel with, *b/a*=1, *b/h*=100, stacking sequence (45°/−45°/−45°/45°) and (0°/90°/90°/0°); subjected to sinusoidal pulse load. Figure 5.14(b) shows the plot of non-dimensional load vs Failure index with respect to Tsai-Wu failure criterion for a panel with, *b/a*=1, *b/h*=100, stacking sequence (45°/−45°/−45°/45°) and

(0°/90°/90°/0°); subjected to sinusoidal pulse load. In Fig.5.13 and Fig. 5.14, solid line represents results of panel with stacking sequence (0°/90°/90°/0°) and dash lines represents results of panel with stacking sequence (45°/-45°/-45°/45°).

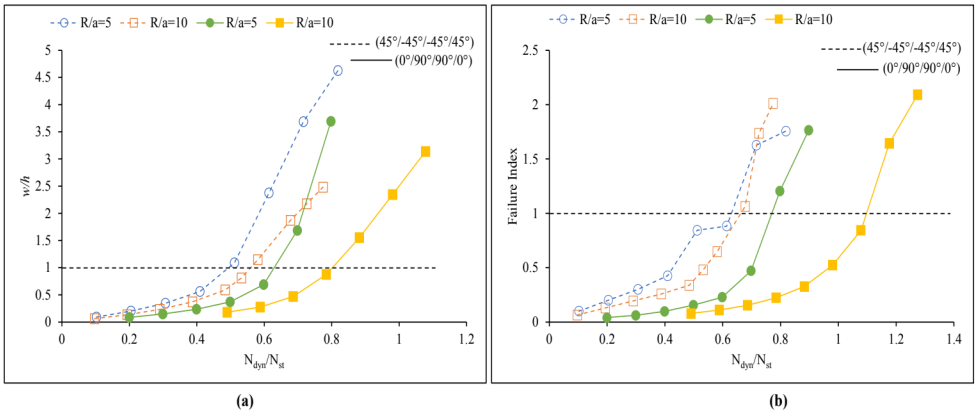

Fig. 5.13 Plot for a laminated composite cylindrical panel with *b/a*=1, *a/h*=100, stacking sequence (45°/−45°/−45°/45°) and (0°/90°/90°/0°) subjected to rectangular pulse load for various *R/a* ratios **(a)** Non-dimensional Load vs non-dimensional Displacement **(b)** Non-dimensional Load vs Failure index (Tsai-Wu criterion)

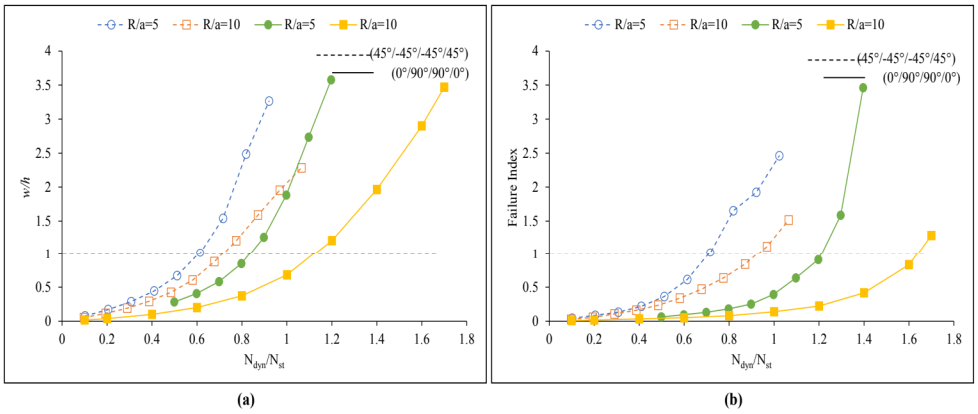

Fig. 5.14 Plot for a laminated composite cylindrical panel with *b/a*=1, *a/h*=100, stacking sequence (45°/−45°/−45°/45°) and (0°/90°/90°/0°) subjected to sinusoidal pulse load for various *R/a* ratios **(a)** Non-dimensional Load vs non-dimensional Displacement **(b)** Non-dimensional Load vs Failure index (Tsai-Wu criterion)

In Fig. 5.13 and Fig. 5.14, N_{st} changes with the change in ply orientation and the radius of curvature of the panel. In Fig. 5.13(a) panel with cross-ply laminates and *R/a*=10 has dynamic

buckling load 12% lower than its static buckling load. for this panel its first ply failure load is higher than its static buckling load. For the rest of the cases, the panel exhibits dynamic buckling load much lower than their static buckling loads. This is observed when the panel is subjected to sinusoidal in-plane pulse loads as well. Panel with angle-ply laminates and *R/a*=10 has dynamic buckling load 12% higher than its static buckling load. for this panel its first ply failure load is also higher than its static buckling load when subjected to sinusoidal pulse load. These results signify that the panel with higher curvature (*R/a*=5) even though has a higher static buckling load, has a lower dynamic buckling load than a panel with lower curvature (*R/a*=10). Panels with lower curvature exhibit better dynamic performance than panels with higher curvatures. Thus, the stiffness and the strength of the panel for in-plane pulse loads increases with the decrease in the curvature of the panel.

Comparing the results of panel subjected to rectangular and sinusoidal pulse loading function, the rectangular pulse loading function will give a higher response since more energy is imparted in the structure. This will be observed in the succeeding section, where the influence of loading function on dynamic buckling behavior of the cylindrical panel is studied.

5.3.5 Effect of loading function

The influence of loading function on the dynamic buckling behaviour of composite cylindrical panel is studied in this section. For this study, for a ratio of *R/a*, three types of aspect ratios (*b/a*=1,2,3) and two types of stacking sequences, the dynamic buckling loads are calculated. The laminated composite cylindrical panel is subjected to rectangular pulse load and sinusoidal pulse load. Figure 5.15(a) shows the plot of non-dimensional load vs non-dimensional displacement for a panel with *R/a*=5, *a/h*=100, stacking sequence (45°/−45°/−45°/45°); for various aspect ratios. Figure 5.15(b) shows the plot of non-dimensional load vs Failure index for a panel with, R/*a*=5, *a/h*=100, stacking sequence (45°/−45°/−45°/45°); with respect to Tsai-Wu failure criterion. Figure 5.16(a) shows the plot of non-dimensional load vs non-dimensional displacement for a panel with R/*a*=5, *a/h*=100, stacking sequence (0°/90°/90°/0°); for various aspect ratios. Figure 5.15(b) shows the plot of non-dimensional load vs Failure index for a panel with, *R/a*=5, *a/h*=100, stacking sequence (0°/90°/90°/0°); with respect to Tsai-Wu failure criterion. In Fig. 5.15 and Fig. 5.16, the codes are represented as aspect ratios. Table 5.3 shows the codes used for different cases. For all cases, simply supported boundary conditions are considered.

Table 5.3 Codes used to represent aspect ratio and loading function in Fig. 5.15 and Fig. 5.16

Code	Aspect Ratio	Pulse Loading Function
Rec_1	*b/a*=1	Rectangular
Rec_2	*b/a*=2	Rectangular
Rec_3	*b/a*=3	Rectangular
Sine_1	*b/a*=1	Sinusoidal
Sine_2	*b/a*=2	Sinusoidal
Sine_3	*b/a*=3	Sinusoidal

The codes described in Table 5.3 are used for better representation of the results in Fig. 5.15 and Fig. 5.16. The solid line in these figures are for the panel subjected to rectangular pulse load and dash line represent the results of the panel subjected to sinusoidal pulse load. In each plot, the value of N_{st} is different for various aspect ratios considered. So, the comparison is made for each aspect ratio separately. The dynamic performance of the panel with *b/a*=1 and stacking sequence (0°/90°/90°/0°) subjected to rectangular pulse load is compared with the panel with the same dimensions and stacking sequence but subjected to sinusoidal pulse load. In other words, in Fig. 5.15(a), the solid blue line is compared with the dashed blue line.

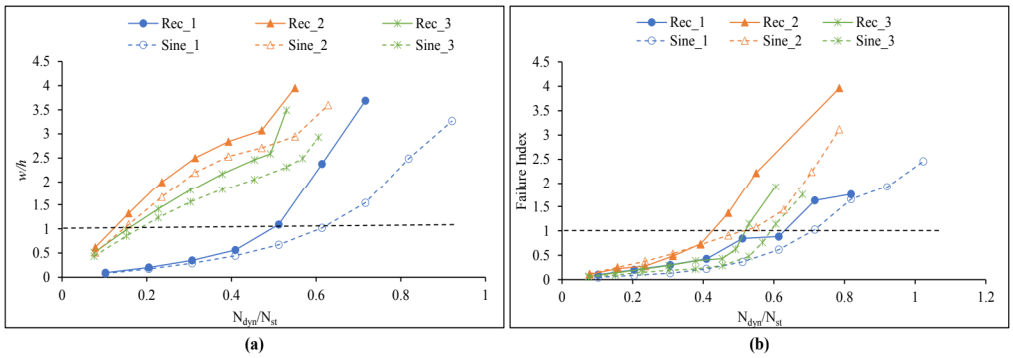

Fig. 5.15 Plot for a laminated composite cylindrical panel with R/*a*=5, *a/h*=100, stacking sequence (45°/−45°/−45°/45°) subjected to rectangular and sinusoidal pulse load for various *b/a* ratios. **(a)** Non-dimensional Load vs non-dimensional Displacement **(b)** Non-dimensional Load vs Failure Index (Tsai-Wu criterion)

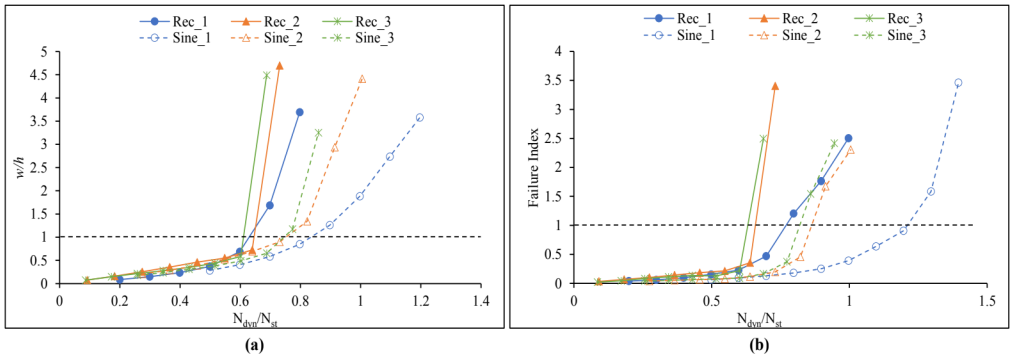

Fig. 5.16 Plot for a laminated composite cylindrical panel with R/*a*=5, *a*/*h*=100, stacking sequence (0°/90°/90°/0°) subjected to rectangular and sinusoidal pulse load for various *b*/*a* ratios. **(a)** Non-dimensional Load vs non-dimensional Displacement **(b)** Non-dimensional Load vs Failure Index (Tsai-Wu criterion)

It is seen from Fig. 5.15(a) and Fig. 5.16(a) that when the composite cylindrical panel is subjected to rectangular pulse load, the non-linear dynamic buckling load is lower than when subjected to sinusoidal pulse load. As the area under the plot of time vs load in the case of a rectangular loading function is higher than that of the sinusoidal load, the panel is subjected to a greater energy when subjected to rectangular loading function. In dynamic loading cases, the duration of loading, as well as the magnitude of load is critical. Hence, rectangular loading function gives a higher response. It is also observed that cross-ply laminates, when subjected to rectangular loading function, will give a sharp rise in response which is due to sudden application and removal of the pulse load. Also, the variation in the behavior of the panel with different aspect ratios is due to the change in the deformation profile of the panel.

Figure 5.17(a) shows the deformed shape of the panel with *b*/*a*=1, *R*/*a*=10, *b*/*h*=100 and stacking sequence (0°/90°/90°/0°) with respect to maximum transverse displacement occurring at the center of the panel when subjected to a rectangular pulse load at which dynamic buckling occurs. Figure 5.17(b) shows the deformed shape of the panel with *b*/*a*=1, *R*/*a*=10, *a*/*h*=100 and stacking sequence (0°/90°/90°/0°) with respect to Tsai-Wu failure criterion occurring near the edge pf the panel when subjected to a rectangular pulse load at which first ply failure occurs. Figure 5.17(c) shows the deformed shape of the panel with *b*/*a*=1, *R*/*a*=10, *a*/*h*=100 and stacking sequence (45°/−45°/−45°/45°) with respect to maximum transverse displacement occurring at the center of the panel when subjected to a rectangular pulse load at which dynamic buckling occurs. Figure 5.17(d) shows the deformed shape of the panel with *b*/*a*=1, *R*/*a*=10,

a/h=100 and stacking sequence (45°/−45°/−45°/45°) with respect to Tsai-Wu failure criterion occurring at the corners of the panel when subjected to a rectangular pulse load at which first ply failure occurs.

Figure 5.18(a) shows the deformed shape of the panel with *b/a*=1, *R/a*=10, *a/h*=100 and stacking sequence (0°/90°/90°/0°) with respect to maximum displacement occurring at the center of the panel when subjected to a sinusoidal pulse load at which dynamic buckling occurs. Figure 5.18(b) shows the deformed shape of the panel with *b/a*=1, *R/a*=10, *a/h*=100 and stacking sequence (0°/90°/90°/0°) with respect to Tsai-Wu failure criterion occurring near the edges when subjected to a sinusoidal pulse load at which first ply failure occurs. Figure 5.18(c) shows the deformed shape of the panel with *b/a*=1, *R/a*=10, *b/h*=100 and stacking sequence (45°/−45°/−45°/45°) with respect to maximum transverse displacement occurring at the center of the panel when subjected to a sinusoidal pulse load at which dynamic buckling occurs. Figure 5.18(d) shows the deformed shape of the panel with *b/a*=1, *R/a*=10, *a/h*=100 and stacking sequence (45°/−45°/−45°/45°) with respect to Tsai-Wu failure criterion occurring at the corners when subjected to a sinusoidal pulse load at which first ply failure occurs.

In the Fig. 5.17 and Fig. 5.18, the scale factor for all the cases is kept 5 for clarity. All the deformed shapes are taken at critical time for maximum value of either displacement or failure index. Also, for all cases, simply supported boundary conditions are considered. It is seen from Fig. 5.17 and Fig. 5.18 that, for the case of panel with stacking sequence (45°/−45°/−45°/45°) ply failure occurs at corner of the panel. And for the case of panel with stacking sequence (0°/90°/90°/0°) ply failure occurs at the center or near the edges. The stresses are varying with the variation of the fiber angles in different layers. For this reason, the failure locations are changing. With the change in stacking sequence and the loading function, the location of first ply failure changes but the location of maximum deformation in the panel at dynamic buckling load does not.

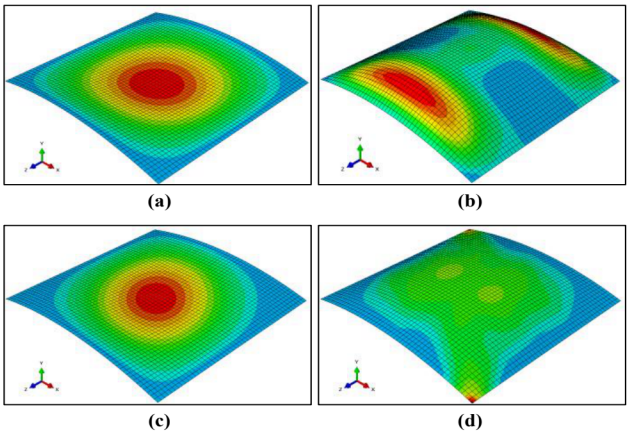

Fig. 5.17 Deformed shape of the laminated composite cylindrical panel with *b/a*=1, *R/a*=10, *a/h*=100, subjected to rectangular pulse load. **(a)** maximum displacement at the center corresponding to loading at which dynamic buckling occurs for a cross-ply laminate **(b)** maximum failure index (Tsai-Wu criterion) corresponding to loading at which first ply failure occurs for a cross-ply laminate **(c)** maximum displacement at the center corresponding to loading at which dynamic buckling occurs for an angle-ply laminate **(d)** maximum failure index (Tsai-Wu criterion) at the corners corresponding to loading at which first ply failure occurs for an angle-ply laminate.

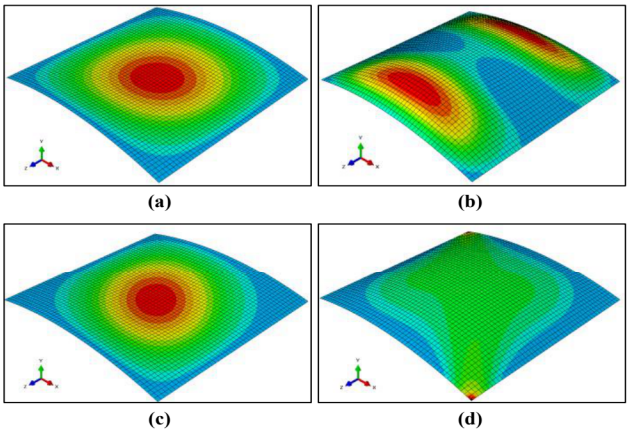

Fig. 5.18 Deformed shape of the laminated composite cylindrical panel with *b/a*=1, *R/a*=10, *a/h*=100, subjected to sinusoidal pulse load. **(a)** maximum displacement at the center corresponding to loading at which dynamic buckling occurs for a cross-ply laminate **(b)** maximum failure index (Tsai-Wu criterion) near the edges corresponding to loading at which first ply failure occurs for a cross-ply laminate **(c)** maximum displacement at the center corresponding to loading at which dynamic buckling occurs for an angle-ply laminate **(d)** maximum failure index (Tsai-Wu criterion) at the corners corresponding to loading at which first ply failure occurs for an angle-ply laminate

5.3.6 Effect of boundary conditions

In this section, the influence of boundary conditions on the dynamic buckling behaviour of cylindrical panel is investigated. Four cases of boundary conditions are considered and the boundary conditions at the loading edges are kept same in all the cases. The various boundary conditions are shown in Fig. 3.7. BC1 refers to all four sides simply supported. BC2 refers to non-loaded edges clamped. BC3 refers to one non-loaded edge clamped, and the other simply supported. BC4 refers to three edges simply supported and one edge free. In all the cases, for the calculation of static buckling load, the boundary conditions are kept same for pre-buckling stage and buckling load calculation.

Laminated composite cylindrical panel with b/a = 1, R/a=5, a/h=100 subjected to rectangular and sinusoidal pulse loads is considered for the investigation. The stacking sequence is (0°/90°/90°/0°) and (45°/-45°/-45°/45°).

Figure 5.19(a) shows the plot of non-dimensional load vs non-dimensional displacement for a panel with b/a=1, R/a=5, a/h=100 subjected to rectangular pulse load for various boundary conditions and stacking sequences. Figure 5.19(b) shows the plot of non-dimensional load vs failure index with respect to Tsai-Wu failure criterion for a panel with b/a=1, R/a=5, a/h=100 subjected to sinusoidal pulse load for various boundary conditions and stacking sequences. Figure 5.20(a) shows the plot of non-dimensional load vs non-dimensional displacement for a panel with b/a=1, R/a=5, a/h=100 subjected to rectangular pulse load for various boundary conditions and stacking sequences. Figure 5.20(b) shows the plot of non-dimensional displacement vs failure index with respect to Tsai-Wu failure criterion for a panel with b/a=1, R/a=5, a/h=100 subjected to sinusoidal pulse load for various boundary conditions and stacking sequences. In Fig.5.19 and Fig. 5.20, solid line represents results for the panel with stacking sequence (0°/90°/90°/0°) and dash lines represents results for the panel with stacking sequence (45°/-45°/-45°/45°).

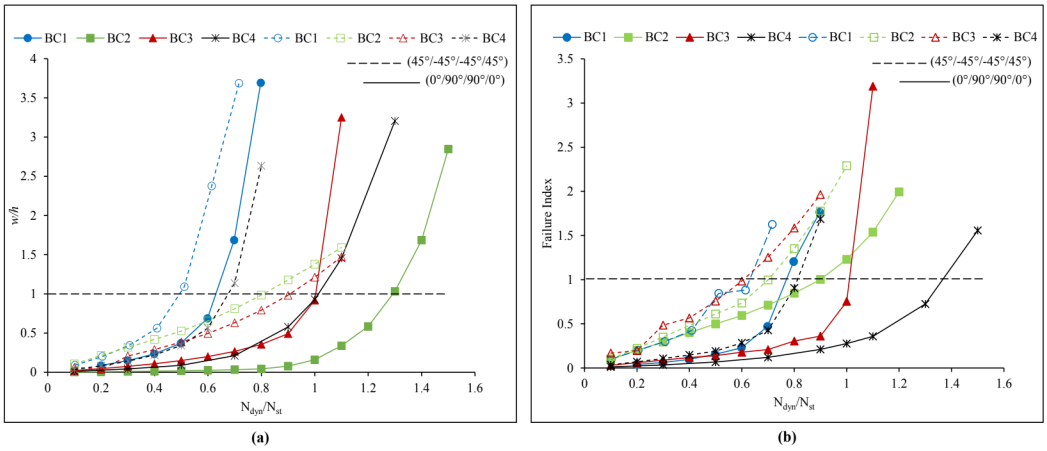

Fig. 5.19 Plot for of the panel with *b/a*=1, *R/a*=5, *a/h*=100, subjected to rectangular pulse load for various stacking sequence and boundary conditions. **(a)**Non-dimensional Load vs non-dimensional Displacement **(b)** Non-dimensional Load vs Failure index (Tsai-Wu criterion)

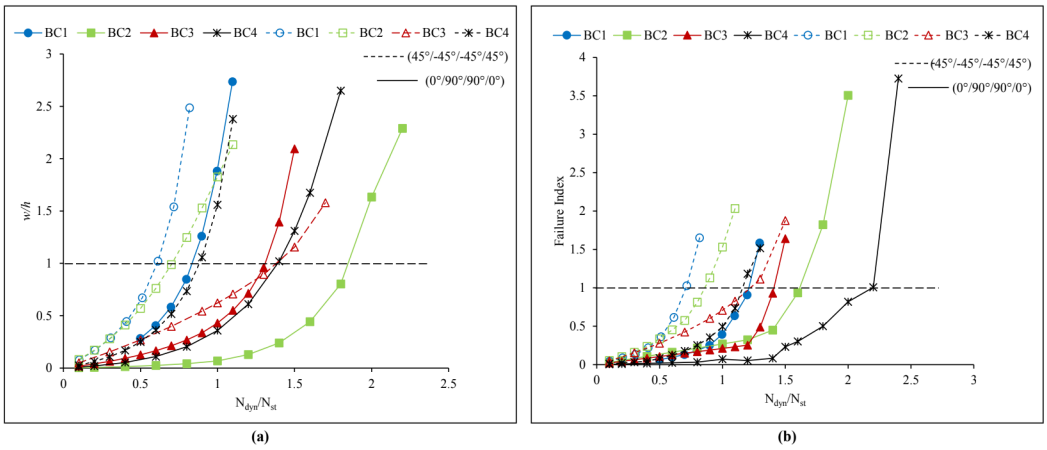

Fig. 5.20 Plot for of the panel with *b/a*=1, *R/a*=5, *a/h*=100, subjected to sinusoidal pulse load for various stacking sequence and boundary conditions. **(a)**Non-dimensional Load vs non-dimensional Displacement **(b)** Non-dimensional Load vs Failure index (Tsai-Wu criterion)

In Fig. 5.19 and Fig. 5.20, the value of Nst changes with the change in the dynamic buckling load. In Fig. 5.19 (a) panel with BC2 and cross-ply laminates has dynamic buckling load 30% higher than its static buckling load when subjected to rectangular in-plane pulse load. For the same laminates with BC3 and BC4, the dynamic buckling loads are equal to their static buckling loads. However, for the panel with angle ply laminates when subjected to rectangular in-plane pulse load have dynamic buckling loads lower than their static buckling loads.

Comparing the panel with the same boundary conditions, the panel with cross-ply laminates have higher strength and stiffness than the panel with angle ply laminates when subjected top rectangular in-plane pulse loads. In Fig. 5.19(b) and 5.20(b), panel with cross-ply laminates and BC4 has the first ply failure load higher than its static buckling load when subjected to rectangular in-plane pulse load (36% higher) or sinusoidal in-plane pulse load (120% higher). The reason for this is that one non-loaded edge of the panel is free. Thus, without constraint, the panel has higher first ply failure load and the panel exhibits higher strength than the other cases. The panel with cross-ply laminates and two non-loaded edges clamped (BC2) exhibits higher stiffness when compared to other boundary conditions.

The variation in the dynamic performance of the panel with different boundary conditions is due to the change in the deformation profile of the panel. The panel has the tendency to deform in a similar manner as its first static buckling mode. With the change in geometry, ply orientation and the boundary conditions, the dynamic performance of the panel is different in each case. It is essential to determine dynamic performance of the panel for various boundary conditions to ascertain the condition for which the panel would have a dynamic buckling load and first ply failure load higher than its static buckling load.

5.4 Shock Spectrum of a Cylindrical Panel

In this section, the shock spectrum of cylindrical panel is presented. For this a balanced and symmetric cross-ply cylindrical panel is considered. The geometric properties are b/a=1, a/h=100, R/a=10. The material properties are presented in Table 3.2. the geometry and the boundary conditions are shown in Fig. 3.6 and Fig. 3.7(a) respectively. For this investigation, the loading functions considered are rectangular, sinusoidal, triangular and exponential shown in Fig. 5.21. In Fig. 5.21(a)-Fig. 5.21(d), the dynamic load is the amplitude of the maximum dynamic load of the loading function. In order to make a comparison, the area under the time vs load plot of each of these figures is kept same. First the static buckling load (18212N/m) and the first natural period (T_n=1.9×10^{-3}s) of the panel are evaluated. Next, the panel is subjected to dynamic load corresponding to three times the static buckling load (N_{dyn}=3×N_{st}) in the form of rectangular pulse load for various durations of loading. The same energy is imparted in the panel in the form of sinusoidal, exponential and triangular pulse loads for various durations of loading. For the same duration of loading, the amplitude of the dynamic load changes for different pulse loading functions. The displacements are non-dimensionalized using the non-linear static displacement by performing Riks analysis corresponding to 3×N_{st}.

The non-linear static displacement (w_{st}) of the panel is 0.0052m. The plot of transverse displacement vs in-plane load for the calculation of w_{st} is shown in Fig. 5.22(a). In the Fig. 5.22 (b) the plot of non-dimensional time vs non-dimensional displacement for the panel subjected to rectangular, sinusoidal, triangular and exponential pulse loads is shown.

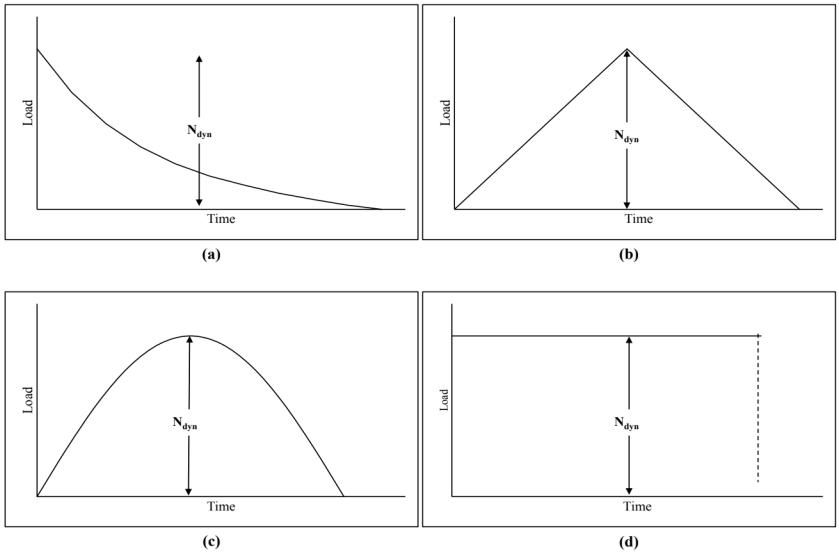

Fig. 5.21 Loading functions considered for shock spectrum **(a)** Exponential pulse load **(b)** Triangular pulse load **(c)** Sinusoidal pulse load **(d)** Rectangular pulse load

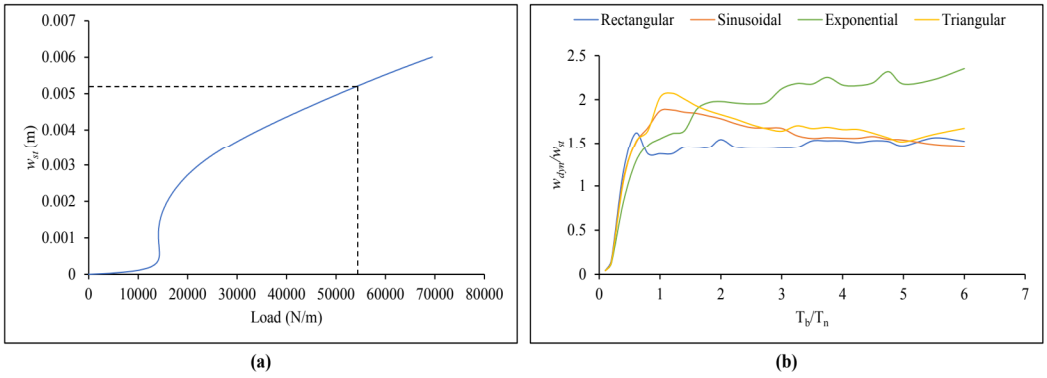

Fig. 5.22 Plot for laminated composite cylindrical panel with R/a=10 and stacking sequence (0°/90°/90°/0°) **(a)** transverse displacement vs in-plane load curve **(b)** Shock Spectrum of the subjected to various pulse loads

In Fig. 5.22, the energy imparted to the cylindrical panel is the same in each case. The duration of loading is kept the same in each case. First the panel is subjected to dynamic load

in the form of rectangular pulse. Then the magnitude of the load is calculated for triangular, sinusoidal and exponential loading functions such that the area under the curve (Fig. 5.21(a)-Fig. 5.21(c)) remains the same in each case. Thus, the magnitude of load is different for each loading type. The lowest magnitude is for rectangular loading function, then sinusoidal loading function followed by triangular loading function and the highest magnitude of dynamic load is for exponential loading function. When the loading duration is very short ($T_b/T_n<0.5$), the maximum response of the system is controlled by the time integral of the pulse area (Chopra, 2007). Thus, the shape of the pulse load has little influence over the response of the panel. This is seen in Fig. 5.22 where, the responses merge when the duration of loading is very short. It is also observed that the response for the panel subjected to rectangular, sinusoidal and the triangular pulse loads stabilize near $T_b/T_n=4$. Panel when subjected to triangular and sinusoidal pulse loads show similar behavior. This is because of the gradual increase and decrease of amplitude of loading in sinusoidal and triangular pulse loading functions. The peaks of the response due to triangular loading function and the sinusoidal loading function are different due to higher rate of increase in dynamic load in case of triangular loading case and also due to higher magnitude of load in triangular loading case. For the case of exponential loading, the response stabilization is much slower than the other cases. In all cases except for exponential pulse load, the maximum displacement occurs near the first natural period of the panel.

5.5 Summary

The dynamic buckling behavior of a laminated composite cylindrical panel subjected to pulse loads is studied in this chapter. The influence of duration of loading, loading function, aspect ratio, curvature, stacking sequence and the boundary conditions on the dynamic buckling behavior of cylindrical panels are studied. The conclusions drawn from the study are presented in Chapter 8 (section 8.4).